9466 *Biochemistry* **2009,** *48,* 9466–9470
DOI: 10.1021/bi900281s

BIOCHEMISTRY
including biophysical chemistry & molecular biology
Article

Functional Energetic Landscape in the Allosteric Regulation of Muscle Pyruvate Kinase. 3. Mechanism[†]

Petr Herman*[,‡,§] and J. Ching Lee*[,§]

[‡]*Faculty of Mathematics and Physics, Institute of Physics, Charles University, Ke Karlovu 5, 121 16 Prague, Czech Republic, and* [§]*Department of Biochemistry and Molecular Biology, University of Texas Medical Branch, Galveston, Texas 77555-1055*

Received February 18, 2009; Revised Manuscript Received July 24, 2009

ABSTRACT: Mammalian pyruvate kinase exists in four isoforms with characteristics tuned to specific metabolic requirements of different tissues. All of the isoforms, except the muscle isoform, exhibit typical allosteric behavior. The case of the muscle isoform is a conundrum. It is inhibited by an allosteric inhibitor, Phe, yet it has traditionally not been considered as an allosteric enzyme. In this series of study, an energetic landscape of rabbit muscle pyruvate kinase (RMPK) was established. The phenomenon of inhibition by Phe is shown to be physiological. Furthermore, the thermodynamics for the temperature fluctuation and concomitant pH change as a consequence of muscle activity were elucidated. We have shown that (1) the differential number of protons released or absorbed with regard to the various linked reactions adds another level of control to shift the binding constants and equilibrium of active ⇆ inactive state changes (the latter controls quantitatively the activity of RMPK); (2) ADP plays a major role in the allosteric mechanism in RMPK under physiological temperatures (depending on the temperature, ADP can assume dual and opposite roles of being an inhibitor by binding preferentially to the inactive form and a substrate); and (3) simulation of the RMPK behavior under physiological conditions shows that the net results of the 21 thermodynamic parameters involved in the regulation are well-tuned to allow the maximal response of the enzyme to even minute changes in temperature and ligand concentration.

Pyruvate kinase, an important glycolytic enzyme, catalyzes a transfer of a phosphate group from phosphoenolpyruvate (PEP) to ADP. This process yields a molecule of pyruvate and ATP. The enzyme has been extensively reviewed by Kayne (*1*). Mammalian PK exists in four isoforms with characteristics tuned to specific metabolic requirements of different tissues (*2*, *3*). All of the isoforms, except the muscle isoform, exhibit typical allosteric behavior. The case of the muscle isoform is a conundrum. It is inhibited by an allosteric inhibitor, Phe, yet it has traditionally not been considered as an allosteric enzyme because the concentration required to elicit demonstrable inhibitory effect is too high to be considered physiological. In this series of study, the goal is to establish an energetic landscape of rabbit muscle pyruvate kinase (RMPK) to resolve this issue of whether the phenomenon of inhibition by Phe is physiological. Furthermore, there is a long-standing interest in the temperature fluctuation and concomitant pH change as a consequence of muscle activity (*4*−*6*). RMPK is being employed as a model system to address the consequences of temperature and pH changes in muscle enzymes.

In the two preceding papers (DOI: 10.1021/bi900279x and 10.1021/bi900280u), we have investigated the tetrameric RMPK. Simultaneous analysis of isothermal titration calorimetry (ITC) data and fluorescence data acquired at different temperatures allowed for thorough thermodynamic characterization of the allosteric regulation of the enzyme within the frame of the two-state concerted model (*7*). According to this model, the RMPK population equilibrates between two states with highly different enzymatic activities. Then the allosteric regulation is achieved by transitions of the RMPK tetramer between the active R and the inactive T state. These concerted conformational transitions of the RMPK subunits can be shifted to favor one state or another by temperature and ligand binding. Besides the thermodynamic characterization of the R ↔ T equilibrium, we also quantified the binding of both RMPK substrates, PEP and ADP, as well as binding of the allosteric inhibitor, Phe.

It was shown that it requires 21 thermodynamic parameters to adequately describe the model for RMPK regulation. These include binding enthalpies and entropies, linked proton reactions, changes in the isothermal heat capacity, ligand interaction parameters, etc. (DOI: 10.1021/bi900280u). Because of the large amount of information, it is difficult to envision behavior of RMPK which is the resultant of the fine interplay among these parameters. In this paper, we present a graphical summary of the previously obtained results with emphasis on the RMPK allosteric regulation. Simulation of the RMPK behavior under physiological conditions shows that all parameters involved in the regulation are well-tuned to allow the maximal response of the enzyme to even minute changes in temperature and ligand concentration.

RESULTS AND DISCUSSION

The foundation of the regulatory mechanism of RMPK is the rapid equilibrium between the two structural states, namely, the active R state and inactive T state. One of the roles of the intricate network of linked reactions is to shift that equilibrium with the exception of a coupling between Phe and ADP bindings. The ability of effectors to regulate the activity is related to their ability to influence the R ↔ T equilibrium. The ability of a ligand

[†]Supported by National Institutes of Health Grant GM 77551 and the Robert A. Welch Foundation (J.C.L.) and Grant MSM 0021620835 of the Ministry of Education, Youth and Sports of the Czech Republic (P.H.).

*To whom correspondence should be addressed. J.C.L.: telephone, (409) 772-2281; fax, (409) 772-4298; e-mail, jclee@utmb.edu. P.H.: telephone, +420-221911461; fax, +420-224922797; e-mail, herman@karlov.mff.cuni.cz.

 Published on Web 08/31/2009

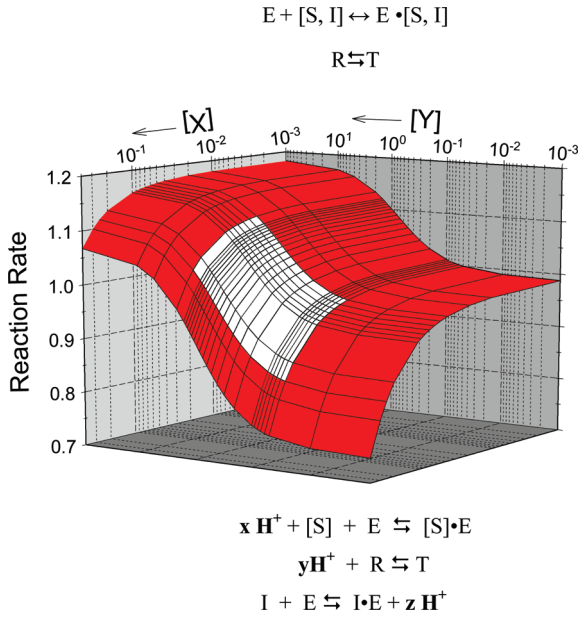

FIGURE 1: Functional energetic landscape of the allosteric regulation of RMPK.

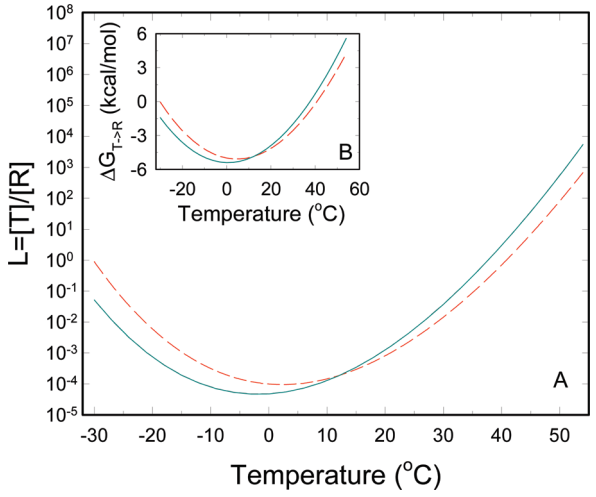

FIGURE 2: Temperature dependence of the R ⇆ T equilibrium of RMPK. (A) Equilibrium constant between the unliganded R and T states in the absence of ligands (cyan solid line) and the apparent one in the presence of 10 mM ADP (red dashed line). (B) Free energy of the T → R transition in the absence of ligands (cyan solid line) and in the presence of 10 mM ADP (red dashed line).

to shift the R ↔ T equilibrium is dependent on the existence of a differential affinity of the ligand for the two states: the greater the difference, the greater the ability to shift the distribution of states. The direction of the shift is dependent on the state to which the ligand binds stronger.

Figure 1 presents a functional energetic landscape of the allosteric regulatory mechanism of RMPK. The landscape is defined by the relationship between two ligands, X and Y, as a function of temperature. The various reactions listed above the landscape represent the reactions that define the function of RMPK, namely, all the reactions of the enzyme with metabolites pertaining to the function of RMPK. The various reactions listed below the landscape indicate the linkage of proton release or absorption to these reactions. Let us review the evidence in support of the mechanism shown in Figure 1.

R ↔ T Equilibrium. A better insight into the apparently complex allosteric regulatory mechanism of the RMPK can be gleaned from a graphical representation of results obtained in the two previous papers by calorimetry and fluorescence techniques (DOI: 10.1021/bi900279x and 10.1021/bi900280u). On the basis of the globally fitted thermodynamic parameters (DOI: 10.1021/bi900280u), the temperature dependence of equilibrium constants underlying the RMPK regulation was calculated. Figure 2A shows the temperature dependence of the R ⇆ T equilibrium constant (L_0 = [T_0]/[R_0]), i.e., ratio of the concentration of inactive T_0 and active R_0 state of the unliganded RMPK. L_0 and its relation with the thermodynamic parameter can be expressed by

$$L_0 = \exp[-(1/RT)(\Delta H_{R\leftrightarrow T} - T\Delta S_{R\leftrightarrow T})] \quad (1)$$

where $\Delta H_{R\leftrightarrow T} = \Delta H_{0,R\leftrightarrow T} + \Delta C_{p,R\leftrightarrow T}(T - T_0)$ and $\Delta S_{R\leftrightarrow T} = \Delta S_{0,R\leftrightarrow T} + \Delta C_{p,R\leftrightarrow T} \ln(T/T_0)$, where R and T are the universal gas constant and the absolute temperature, respectively. Figure 2A shows a bell-shaped relation between temperature and L_0, exhibiting a minimum near 0 °C. The observed minimum stems from a positive isobaric heat capacity change ($\Delta C_{p,R\leftrightarrow T}$) of 2.2 kcal/mol. The consequence of the bell-shaped relation is to ensure that L_0 is more sensitive to fluctuations of temperature at physiologically relevant temperatures. In turn, the activity of RMPK is most responsive to temperature since the enzyme activity is directly related to the distribution of the active R and inactive T states.

Under temperatures where L_0 assumes the minimum value, it means that there is a negligible amount of RMPK in the inactive T state; i.e., essentially all of RMPK is in the R state at low temperatures. As the temperature increases, the value of L_0 increases, indicating that the distribution between the R and T states becomes more toward the T state. The favorable shift toward the R state at low temperatures is the basis for the observation that RMPK exhibits a hyperbolic kinetic behavior in the absence of inhibitor at temperatures below room temperature (*8*).

To improve our understanding of the influence of temperature on the RMPK regulation, it is practical to visualize temperature-induced changes in the fraction of inactive state f^T in the absence and in the presence of ligands. The fractions, as shown in Figure 3A, were calculated from the corresponding equilibrium constants between the R and T states as

$$f^T = L/(1+L) \quad (2)$$

where L is equal to L_0 or $L_{0,lig}$ for the unliganded or RMPK saturated by the ligand (DOI: 10.1021/bi900279x), respectively. The value of f^T for unliganded RMPK is bell-shaped with a negligible fraction of the inactive state between −25 and 25 °C. The shape of the curve is governed by the temperature dependence of L_0, as shown in Figure 2. Above 30 °C, the value of f^T starts to sharply increase and the R → T transition is almost completed at 40 °C.

PEP Binding. Values of K_{lig}^R or K_{lig}^T, the microscopic binding constant of ligand to the R or T state, respectively, can be calculated according to the equation

$$\ln(K_{lig}^{state}) = 1/R(\Delta H_{lig}^{state}/T - \Delta S_{lig}^{state}) \quad (3)$$

where binding enthalpies ΔH_{lig}^{state} and entropies ΔS_{lig}^{state} are results of the global fitting presented in the preceding paper (DOI: 10.1021/bi900280u). Figure 4 shows the K_d values of RMPK for PEP as a function of temperature. Binding of PEP to the R state shows a slight temperature dependence due to a ΔH_{PEP}^R of −2.1 kcal/mol. Negative enthalpy terms indicate weaker

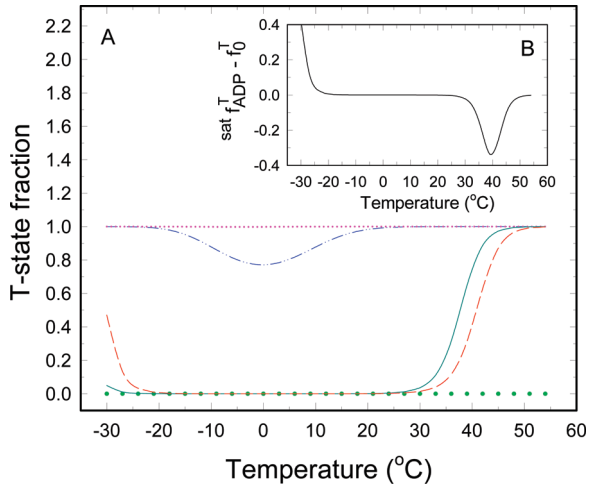

FIGURE 3: Temperature dependence of the T state fraction of RMPK. (A) T state fraction for unliganded RMPK (cyan solid line), for RMPK saturated with 10 mM ADP (red dashed line), 12 mM Phe (pink dotted line), or 2 mM PEP (green small circles), and for RMPK in the presence of both 12 mM Phe and 10 mM ADP (blue dashed−dotted line). (B) Difference between the T state fraction of RMPK in the presence of 10 mM ADP and the T state fraction of the unliganded RMPK.

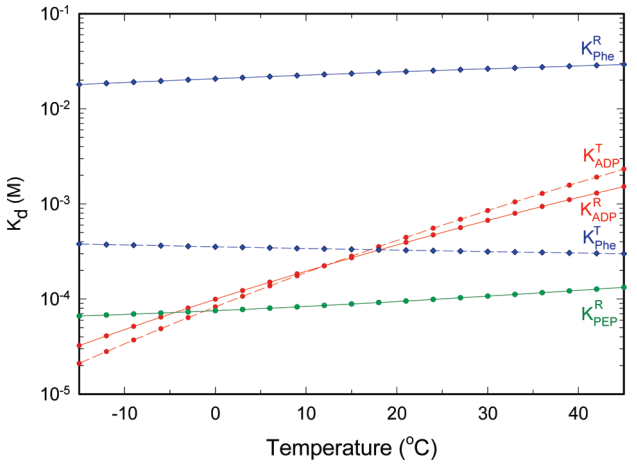

FIGURE 4: Temperature dependence of dissociation constants for PEP (green line), ADP (red lines), and Phe (blue lines). The solid and dashed lines represent binding to the R and T states of PK, respectively.

binding of the ligand at elevated temperatures. The binding of PEP to the T state is significantly weaker, so much so that no accurate value can be derived from this series of study, although results based on steady state kinetics imply a ≥10-fold weaker affinity (*8*).

Differential binding affinities of a ligand toward the R and T states, K^R_{lig} and K^T_{lig}, respectively, result in a shift of the R ↔ T equilibrium as a consequence of the relationship

$$L_{0,\,lig} = L_0(K^R_{lig}/K^T_{lig})^4 \qquad (4)$$

where $L_{0,lig}$ is L_0 in the presence of a saturating amount of ligand (*4*, *5*). Furthermore, a differential temperature dependence of these affinities causes the shift to be temperature-dependent as well. Since $K^R_{PEP} < K^T_{PEP}$ at all temperatures, binding of PEP will always shift RMPK toward the active R state, a prediction substantiated by the results of steady state kinetics (*8*).

We also investigated a temperature dependence of the T state fraction of RMPK in the presence of a saturating amount of PEP.

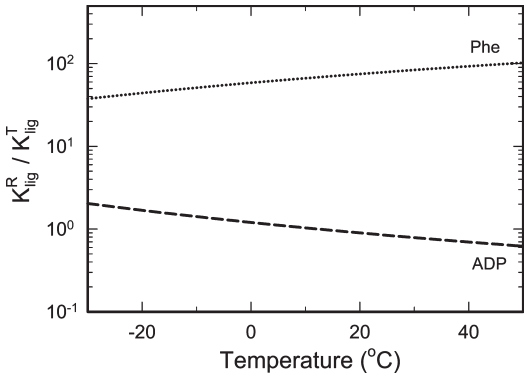

FIGURE 5: K^R_{lig}/K^T_{lig} ratio between dissociation constants from the R and T states of RMPK for ADP (dashed line) and Phe (dotted line) as a function of temperature.

The calculated temperature dependence is depicted in Figure 3A by the empty circles (f^T_{PEP}). It is seen that at all investigated temperatures the presence of a saturating amount of PEP keeps the entire RMPK population in the active R state.

Phe Binding. The temperature dependence of dissociation constants for Phe is shown in Figure 4. Phe binding to both states exhibits only weak temperature dependence that is characterized by a relatively small binding enthalpy change (ΔH^R_{Phe}) of −1.4 kcal/mol and a ΔH^T_{Phe} of 0.65 kcal/mol. The differential binding affinity as a function of temperature can be expressed as the K^R_{Phe}/K^T_{Phe} ratio, as shown in Figure 5. The affinity of Phe for the T state is greater than that for the R state at all investigated temperatures, as shown in Figure 4; thus, the K^R_{Phe}/K^T_{Phe} ratio is always greater than 1. Since K^T_{Phe} is more favored by a higher temperature than K^R_{Phe}, the ratio increases with temperature, as shown in Figure 5. Therefore, Phe always acts as an allosteric inhibitor by shifting the RMPK population to the inactive T state, particularly at higher temperatures.

The temperature dependence of the T state fraction of RMPK in the presence of a saturating amount of Phe is shown in Figure 3A as the dotted line (f^T_{Phe}). Similar to the case of PEP binding, saturation of RMPK by Phe in the absence of other ligands shifts the RMPK population fully to the inactive T state regardless of temperature.

ADP Binding. ADP appears to be an intriguing allosteric effector. The value of K^R_{ADP} increases more than 10-fold between 0 and 40 °C. K^T_{ADP} is even more temperature sensitive, as shown in Figure 4. At 23 °C, K^R_{ADP} = 450 μM, a value in good agreement with a result obtained from steady state kinetics (*9*). The strong increase in the ADP dissociation constants with an increase in temperature is caused by significantly larger binding enthalpies for ADP (ΔH^R_{ADP} = −10.5 kcal/mol, and ΔH^T_{ADP} = −12.8 kcal/mol) than for PEP or Phe. The R state is therefore slightly disfavored by the ADP binding. The unfavorable free energy change was found to be 0.3 kcal/4 = 75 cal/monomer of RMPK (Figure 1B).

According to the model described previously (DOI: 10.1021/bi900279x and 10.1021/bi900280u), the equilibrium constant in the presence of ADP can be calculated as

$$L_{0,\,ADP} = L_0(1+[ADP]/K^T_{ADP})^4/(1+[ADP]/K^R_{ADP})^4 \qquad (5)$$

where K^T_{ADP} and K^R_{ADP} are microscopic dissociation constants of ADP from the T and R states, respectively. The equation shows that any differential affinity of ADP for the R and T states, i.e., any difference in K^R_{ADP} and K^T_{ADP}, will cause a shift of the R ↔ T

equilibrium. Because both K^{T}_{ADP} and K^{R}_{ADP} are temperature-dependent

$$K^{state}_{lig} = \exp[(1/RT)(\Delta H^{state}_{lig} - T\Delta S^{state}_{lig})] \quad (6)$$

the shift of the equilibrium will depend on temperature as well.

The calculated temperature dependence of $L_{0,ADP}$ is depicted in Figure 2A. One can see that in the presence of 10 mM ADP the $L_{0,ADP}$ minimum shifts several degrees Celsius to a higher temperature, compared to the equilibrium constant L_0. As described above, this shift is caused by a difference between K^{R}_{ADP} and K^{T}_{ADP}.

As seen in Figure 5, the ratio of the dissociation constants (K^{R}_{ADP}/K^{T}_{ADP}) decreases with an increase in temperature. The ratio actually crosses over from >1 to <1 with an increase in temperature; i.e., the relative affinities for the R and T states are reversed. The ratio equals 1 near 12 °C. At this temperature, the presence of ADP does not influence the R ↔ T equilibrium. At >12 °C, ADP binds preferentially to the R state and exerts an activating effect on RMPK by shifting the enzyme population to the active R state. At <12 °C, ADP acts as an allosteric inhibitor. In conclusion, depending on the temperature, ADP induces either activation or inhibition of RMPK.

For RMPK saturated with ADP, the transition from the R to T state shifts ~3 °C to a higher temperature, as shown in Figure 3A. Figure 3A further suggests that the ADP-induced redistribution of the RMPK states becomes important mainly in two rather narrow temperature regions around −20 and 40 °C. Figure 3B expresses the data as $^{sat}f^{T}_{ADP} - f^{T}_{0}$, where $^{sat}f^{T}_{ADP}$ and f^{T}_{0} are the T state fractions in the presence and absence of ADP, respectively. The difference $^{sat}f^{T}_{ADP} - f^{T}_{0}$ is explicitly shown in Figure 3B. It is seen that the physiologically relevant region is located between 30 and 45 °C where the presence of ADP causes strong RMPK activation. Specifically, it is seen that at ~40 °C almost 35% of the RMPK population converts from the inactive to the active state in the presence of ADP. Interestingly, the rabbit physiological temperature of ~39 °C falls into this temperature interval (*10*, *11*). The second temperature region of the significant ADP effect can be found at sub-zero temperatures, where ADP causes RMPK inactivation by an increase in the T state fraction. At other temperatures, ADP does not seem to significantly influence the allosteric regulation of RMPK. This observation is consistent with results of Consler et al. who did not detect any effect of ADP on the allosteric properties of RMPK at 23 °C (*9*). Although the inhibition of RMPK by ADP at temperatures below −20 °C is probably physiologically irrelevant, the described mechanism of switching between activation and inhibition is general for any two-state concerted system. Depending on the temperature and the associated thermodynamic parameters, ligands can activate or inhibit enzymes. Because the switching temperature between the activation and inactivation is determined by a fine interplay of the thermodynamic binding parameters, the described effect could be important for other allosteric proteins.

Our data presented in the preceding paper (DOI: 10.1021/bi900280u) suggest that at low temperatures an addition of a saturating amount of ADP to RMPK, which is fully inhibited by Phe, would lead to an allosteric activation of RMPK. The activation is the result of a decrease in the fraction of the T state in the presence of both Phe and ADP. A calculated temperature dependence of f^{T} under these conditions is shown in Figure 3A by the dashed−dotted line. The presence of 10 mM ADP causes a decrease in f^{T} in the temperature range from −20 to 20 °C even in the presence of 12 mM Phe. In the absence of ADP, we predict that at this Phe concentration RMPK is inactive as shown in Figure 3A.

Role of Protonation and Deprotonation. In this study of RMPK, it has been shown that protons are released or absorbed in these linked reactions, as shown in Figure 1. These linked reactions of proton release or absorption may play an equally important role in modulating the allosteric behavior of RMPK. For the reactions that involve proton release, a lower pH would shift the equilibria to the left, as defined by Le Chatelier's principle. Thus, a lower pH would strengthen the binding of ADP and PEP and favor the T state. The net result would be an expected change in the cooperativity of substrate binding. This may be particularly relevant to the normal behavior of RMPK. It has long been reported that the development of acidosis is associated with intense exercise (*12*−*15*). Furthermore, intense exercise can lead to an increase in temperature (*20*). An increase in muscle temperature causes stronger RMPK activation, and a temperature decrease causes RMPK inactivation compared to the reference state without ADP. Thus, under intense exercise, the conditions would favor a higher activity of RMPK to generate additional ATP.

RMPK Regulatory Behavior under Physiological Conditions. Having thermodynamically characterized the regulatory mechanism of RMPK, we were interested in simulating the state distribution under physiological conditions when both ADP and PEP are present in solution. It was shown that in a resting skeletal muscle the PEP and ADP concentrations are close to 30 and 50 μM, respectively (*16*). At the rabbit physiological temperature of ~39 °C, both values are significantly lower than their corresponding dissociation constants [K^{R}_{PEP} = 120 μM, and K^{R}_{ADP} = 1.1 mM (Figure 4)]. Under these conditions, only a small population of RMPK subunits simultaneously binds both substrates that are required for enzymatic activity. As a consequence, only low reaction rates are observed. While the PEP concentration does not change significantly during muscle contraction, the ADP concentration increases primarily due to the shift in the following equilibrium

$$\text{ADP+creatine−P} \leftrightarrows \text{ATP+creatine}$$

that is maintained by creatine kinase. Because creatine phosphate is consumed during muscle contraction, the reaction equilibrium is displaced toward higher ADP concentrations. During intense muscle activity, the ADP concentration can increase to almost 3 mM (*17*−*19*). According to the data from Figures 2 and 3, the increased ADP concentration not only causes RMPK activation but also changes the apparent cooperativity of the PK-catalyzed reaction. Both effects result from the ADP-induced shift in the R ↔ T equilibrium. To investigate the influence of temperature and ADP concentration on the state distribution, we plotted the change in the fraction of the R state, Δf^{R}, upon addition of a variable amount of ADP ($\Delta f^{R} = f^{R}_{ADP} - f^{R}_{withoutADP}$) at different temperatures. The simulation was conducted in the presence of a physiological PEP concentration of 30 μM. The apparent equilibrium constant needed for calculation of $f^{R} = 1/(1 + L)$ in the presence of both PEP and ADP was calculated as

$$L_{0,ADP,PEP} = L_0 \left(\frac{1+[ADP]/K^{T}_{ADP}}{1+[ADP]/K^{R}_{ADP}}\right)^4 \left(\frac{1+[PEP]/K^{T}_{PEP}}{1+[PEP]/K^{R}_{PEP}}\right)^4 \quad (7)$$

Because binding of PEP to the T state was found to be very weak (DOI: 10.1021/bi900280u), i.e., the physiological PEP

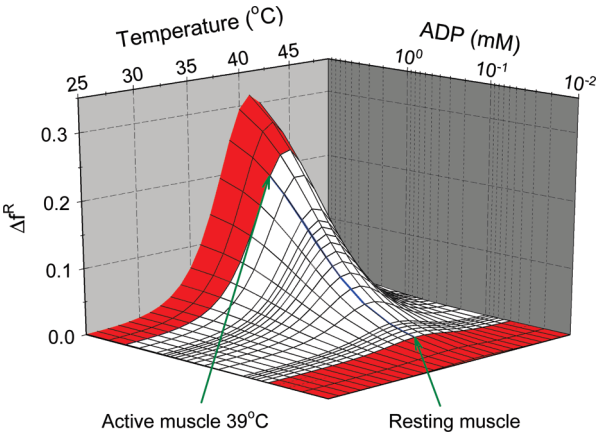

FIGURE 6: Predicted effect of ADP on the activation of the rabbit muscle PK in the presence of a physiological concentration of PEP (30 μM). $\Delta f^{R} = f^{R}_{ADP} - f^{R}_{withoutADP}$ is an increase in the active R state fraction upon addition of ADP. The white section is the approximate region of physiological ADP concentrations. The blue line is the isotherm at 39 °C.

concentration is always much lower than the value of K^{T}_{PEP}, the equation can be approximated by

$$L_{0,\,ADP,PEP} = L_0 \left[\frac{1+[ADP]/K^{T}_{ADP}}{(1+[ADP]/K^{R}_{ADP})(1+[PEP]/K^{R}_{PEP})} \right]^4 \quad (8)$$

The result of the simulation is depicted in Figure 6, where the estimated region of the physiological ADP concentrations is colored white. Figure 6 reveals that near the physiological temperature of rabbit at 39 °C an intense muscle contraction would result in a peak of almost 3 mM ADP which would induce an ~20% increase in the fraction of active state RMPK.

In conclusion, we have shown the following.

1 Equilibrium constants involved in the allosteric regulatory mechanism of RMPK are fine-tuned to facilitate the maximal response of the enzyme to even minute changes in temperature and ligand concentration.

2 The differential number of protons released or absorbed with regard to the various linked reactions adds another level of control to shift the binding constants and R ↔ T equilibrium, which controls quantitatively the activity of RMPK.

3 ADP was shown to be an important allosteric effector significantly affecting the allosteric regulation of RMPK. The ADP action was shown to be highly temperature-dependent. Any ligand of any enzyme can behave like ADP in RMPK, i.e., can under favorable conditions exert either an activating or inhibitory effect.

ACKNOWLEDGMENT

We thank Drs. X. Cheng and A. Gribenko for critical review of the manuscript. This series of papers is dedicated to Professor Serge N. Timasheff who taught us the beauty and power of thermodynamics of linked reactions in biology.

REFERENCES

1. Kayne, F. (1973) Pyruvate kinase. In The Enzymes (Boyer, P. D., Ed.) 3rd ed., p 353, Academic Press, New York.
2. Bigley, R. H., Koler, R. D., and Richterich, R. (1974) Regulatory properties of three human pyruvate kinases. *Enzyme 17*, 297–306.
3. Boivin, P., and Galand, C. (1974) A mutant of human red cell pyruvate kinase with high affinity for phosphoenolpyruvate. *Enzyme 18*, 37–47.
4. Kemp, G., Boning, D., Beneke, R., and Maassen, N. (2006) Explaining pH change in exercising muscle: Lactic acid, proton consumption, and buffering vs. strong ion difference. *Am. J. Physiol. 291*, R235–R237.
5. Reeves, R. B. (1977) The interaction of body temperature and acid-base balance in ectothermic vertebrates. *Annu. Rev. Physiol. 39*, 559–586.
6. Stevens, E. D., and Godt, R. E. (1990) Effects of temperature and concomitant change in pH on muscle. *Am. J. Physiol. 259*, R204–R209.
7. Monod, J., Wyman, J., and Changeux, J. P. (1965) On the Nature of Allosteric Transitions: A Plausible Model. *J. Mol. Biol. 12*, 88–118.
8. Consler, T. G., Jennewein, M. J., Cai, G. Z., and Lee, J. C. (1992) Energetics of Allosteric Regulation in Muscle Pyruvate Kinase. *Biochemistry 31*, 7870–7878.
9. Consler, T. G., Jennewein, M. J., Cai, G. Z., and Lee, J. C. (1990) Synergistic effects of proton and phenylalanine on the regulation of muscle pyruvate kinase. *Biochemistry 29*, 10765–10771.
10. Gonzalez, R. R., Kluger, M. J., and Hardy, J. D. (1971) Partitional calorimetry of the New Zealand white rabbit at temperatures 5−35 °C. *J. Appl. Physiol. 31*, 728–734.
11. McEwen, G. N., Jr., and Heath, J. E. (1973) Resting metabolism and thermoregulation in the unrestrained rabbit. *J. Appl. Physiol. 35*, 884–886.
12. Robergs, R. A., Ghiasvand, F., and Parker, D. (2004) Biochemistry of exercise-induced metabolic acidosis. *Am. J. Physiol. 287*, R502–R516.
13. Adams, G. R., Foley, J. M., and Meyer, R. A. (1990) Muscle buffer capacity estimated from pH changes during rest-to-work transitions. *J. Appl. Physiol. 69*, 968–972.
14. Kemp, G. J., Taylor, D. J., Styles, P., and Radda, G. K. (1993) The production, buffering and efflux of protons in human skeletal muscle during exercise and recovery. *NMR Biomed. 6*, 73–83.
15. Kushmerick, M. J. (1997) Multiple equilibria of cations with metabolites in muscle bioenergetics. *Am. J. Physiol. 272*, C1739–C1747.
16. Kerson, L. A., Garfinkel, D., and Mildvan, A. S. (1967) Computer simulation studies of mammalian pyruvate kinase. *J. Biol. Chem. 242*, 2124–2133.
17. Dawson, M. J., Gadian, D. G., and Wilkie, D. R. (1978) Muscular fatigue investigated by phosphorus nuclear magnetic resonance. *Nature 274*, 861–866.
18. Nagesser, A. S., Van der Laarse, W. J., and Elzinga, G. (1993) ATP formation and ATP hydrolysis during fatiguing, intermittent stimulation of different types of single muscle fibres from *Xenopus laevis*. *J. Muscle Res. Cell Motil. 14*, 608–618.
19. Westerblad, H., and Lannergren, J. (1994) Changes of the force-velocity relation, isometric tension and relaxation rate during fatigue in intact, single fibres of *Xenopus* skeletal muscle. *J. Muscle Res. Cell Motil. 15*, 287–298.
20. Kenny, G. P., Reardon, F. D., Zaleski, W., Reardon, M. L., Haman, F., and Ducharme, M. B. (2003) Muscle temperature transients before, during, and after exercise measured using an intramuscular multisensor probe. *J. Appl. Physiol. 94*, 2350–2357.